MRI Imaging & Applications

7T Small Bore Scanner

TCIN MRI Imaging Facility

The TCIN MRI centre is a national facility available through an online booking system and at equivalent costs to TCD researchers https://www.tcd.ie/Neuroscience/technologies/access.php
Although very widely used in aging research and other neurodegenerative and neurodevelopmental research at TCIN , it has from the start been open to all disciplines as befitting such a versatile non-invasive research technique.

- The 7T scanner has been used in many different fields (other than Brain research) from **nano/bio/pharma** materials development to cancer research.
- It has triggered collaborations between scientists with interests in the life sciences and scientists in Physics/Chemistry and nanoscience with the objective of developing novel MRI contrast agents and biomarkers for illness.
- It facilitates early-stage visualization of translational research (for example in the development of therapeutics for Retinitis Pigmentosa with colleagues in Genetics)
- It provides the infrastructure to train PhD students, postdoctoral fellows, research support staff and PIs (funded through EU ITN, HRB & other programmes)
- Open for novel technique development at nominal costing (Pilot scan procedure)

Technical Specifications

The 7T MRI lab houses an actively shielded Bruker BioSpec 70/30 USR 7T system with the Bruker AVANCE III HD architecture and Paravision 6 Software. This state-of-the-art scanner can reach a spatial resolution of 25 microns. Available RF-probes include a 1H MRI Cryoprobe, and a 1H receive-only 8 x 1 rat head surface array coil.

Gradients available include:

- BGA 20 (200 mT/m, ID 200 mm)
- BGA 12 (400 mT/m, ID 120 mm)
- BGA 9S (675mT/m, ID 90 mm)
- BGA 6 (1000 mT/m, ID 60 mm)

(ID = maximum usable internal diameter)

Methods currently used on the 7T system include:

- 'Conventional' MR images based on T 1, T 2 or proton density, typically used to show anatomical detail;
- Blood flow in arteries or veins (magnetic resonance angiography or MRA);
- Blood perfusion through tissue, giving cerebral blood flow (CBF) and cerebral blood volume (CBV) maps;
- Molecular diffusion of water through tissue such as white matter tracts (tractography and diffusion tensor imaging (DTI));
- Relative degrees of bound and unbound water via magnetization transfer contrast (MTC);
- Tissue movement, such as motion of the heart to yield measures of ejection fraction and myocardial wall motion;
- Tissue temperature and intracellular pH measurements;
- Oxygenation of blood to show areas of brain activated by stimuli - functional MRI (fMRI);
- Changes in blood perfusion through tissues responding to pharmacological intervention (phMRI);
- Cell tracking following the labelling of cells with magnetic nanoparticles.
- Multi-nuclei spectroscopy and imaging is possible.

7T MRI in Aging research

High-resolution anatomical MRI scans of young and aged rats revealed significant loss of grey matter signal in specific areas of the cortex and hippocampus with no detectable loss of signal in areas such as the thalamus or cerebellum.
Blau CW, Cowley TR, O'Sullivan J, Grehan B, Browne TC, Kelly L, Birch A, Murphy N, Kelly AM, Kerskens CM, Lynch MA. (2012) The age-related deficit in LTP is associated with changes in perfusion and blood-brain barrier permeability. Neurobiol Aging. 33(5):1005.e23-35. doi: 10.1016/j.neurobiolaging.2011.09.035.

Relaxometry

Longitudinal (T1) and transverse (T2) relaxation times are measures of the time taken for the magnetization of water protons to revert back to equilibrium, following radio frequency excitation. T2*, the observed time constant of the free induction decay, is a measure of the combination of magnetic field in-homogeneities and transverse relaxation times. Both T1 and T2 times are tissue-specific, and all three are dependent on the biophysical and chemical properties of tissue. By altering the timepoint of MRI signal acquisition during relaxation, contrast can be created between different tissue types.

T1-, T2 and T2*-weighted images allow visualization of different structures within the brain. Relaxometry involves the acquisition the T1, T2 or T2* relaxation **time** of each voxel in the image. These relaxation times have been proposed as methods of longitudinally assessing the status of brain tissue.

Applications:
The overarching aim of ongoing work is to increase our understanding of the link between changes in MRI relaxometry and inflammatory changes in the brain of aged animals, lipopolysaccharide-treated and amyloid-β-treated animals, as well as animal models of neurodegenerative diseases. There is evidence which suggests a correlation between T1 relaxation time and activation of astrocytes, and between T2 relaxation and microglial activation.

McIntosh A, Mela V, Harty C, Minogue AM, Costello DA, Kerskens C, Lynch MA. (2019) Iron accumulation in microglia triggers a cascade of events that leads to altered metabolism and compromised function in APP/PS1 mice. Brain Pathol. 29(5):606-621. doi: 10.1111/bpa.12704.

Cowley TR, O'Sullivan J, Blau C, Deighan BF, Jones R, Kerskens C, Richardson JC, Virley D, Upton N, Lynch MA.(2012) Rosiglitazone attenuates the age-related changes in astrocytosis and the deficit in LTP. Neurobiol Aging. 33(1):162-75. doi: 10.1016/j.neurobiolaging.2010.02.002.

Bolus tracking arterial spin labeling (ASL)

Arterial spin labeling (ASL) uses inflowing magnetically-labeled arterial water as an endogenous contrast agent in the brain. A new non-compartmental model of cerebral perfusion, based on a Fokker-planck equation, has been developed.

Solutions to the Fokker-Planck equation have been found for the initial conditions of the various ASL techniques. Mean transit times (MTT), capillary transit times (CTT), relative cerebral blood flow and volume (rCBF and rCBV) and the perfusion coefficient, P, can be quantified by performing a least-squares fit of the model to ASL data.

Variations in these perfusion parameters under varying physiological and pathophysiological conditions are of interest in both the research and clinical setting.

Analysis using this method has revealed an age-related decrease in cerebral perfusion and ongoing experiments are directed at assessing whether these changes can be modulated by different treatments. Transient increases in cerebral perfusion have been identified in animals following methylendioxymethamphetamine (MDMA; 'Ecstasy') administration and have been shown to accompany neuronal activation in the somatosensory cortex.

Kelly ME, Blau CW, Kerskens CM (2009) Bolus-tracking arterial spin labeling: theoretical and experimental results. *Physics in Medicine and Biology*, 54:1235-1251.

Gormley S, Rouine J, McIntosh A, Kerskens C, Harkin A. (2016) Glial fibrillary acidic protein (GFAP) immunoreactivity correlates with cortical perfusion parameters determined by bolus tracking arterial spin labelling (bt-ASL) magnetic resonance (MR) imaging in the Wistar Kyoto rat. Physiol Behav. 160:66-79. doi: 10.1016/j.physbeh.2016.04.007.

Rouine J, Kelly ME, Jennings-Murphy C, Duffy P, Gorman I, Gormley S, Kerskens CM, Harkin A. (2015) Investigation of the mechanisms mediating MDMA "Ecstasy"-induced increases in cerebro-cortical perfusion determined by btASL MRI. Psychopharmacology (Berl). 232(9):1501-13. doi: 10.1007/s00213-014-3790-0.

Rouine J, Gobbo OL, Campbell M, Gigliucci V, Ogden I, McHugh Smith K, Duffy P, Behan B, Byrne D, Kelly ME, Blau CW, Kerskens CM, Harkin A. (2013) MDMA 'ecstasy' increases cerebral cortical perfusion determined by bolus-tracking arterial spin labelling (btASL) MRI. Br J Pharmacol. 169(5):974-87. doi: 10.1111/bph.12178.

Functional MRI (fMRI)

ASL (with the appropriate anaesthetic, which has been identified from a panel of anaesthetic protocols) enables non-invasive imaging of the same animal and measurement of the brain response to peripheral electrical stimulation over time.

Kelly ME, Blau CW, Griffin KM, Gobbo OL, Jones JF, Kerskens CM. (2010) Quantitative functional magnetic resonance imaging of brain activity using bolus-tracking arterial spin labeling. J Cereb Blood Flow Metab. 30(5):913-22. doi: 10.1038/jcbfm.2009.284.

Griffin KM, Blau CW, Kelly ME, O'Herlihy C, O'Connell PR, Jones JF, Kerskens CM. (2010) Propofol allows precise quantitative arterial spin labelling functional magnetic resonance imaging in the rat. Neuroimage. 51(4):1395-404. doi: 10.1016/j.neuroimage.2010.03.024.

Contrast MRI

Contrast agents are commonly used to enhance MR signal, to delineate areas of pathology (e.g. infarction, neoplasia), to measure relative cerebral blood volume (rCBV), and to assess blood-brain barrier (BBB) permeability.

(a) BBB permeability has been assessed using intravenous injections of standard gadolinium-based contrast agents. The evidence suggests that MDMA administration leads to an acute, transient opening of the BBB and also when the tight junction protein, claudin-5, is downregulated by siRNA. Using this technique, an age-related increase in rCBV, without BBB permeability changes, has been identified in the rat.

Campbell M, Kiang AS, Kenna PF, Kerskens C, Blau C, O'Dwyer L, Tivnan A, Kelly JA, Brankin B, Farrar GJ, Humphries P. (2008) RNAi-mediated reversible opening of the blood-brain barrier. J Gene Med. 10(8):930-47. doi: 10.1002/jgm.1211.

Christoph W Blau, Thelma R Cowley, Joan O'Sullivan, Belinda Grehan, Tara C Browne, Laura Kelly, Amy Birch, Niamh Murphy, Aine M Kelly, Christian M Kerskens, Marina A Lynch (2012) The age-related deficit in LTP is associated with changes in perfusion and blood-brain barrier permeability. Neurobiol Aging 33(5):1005.e23-35. doi: 10.1016/j.neurobiolaging.2011.09.035.

(b) Smaller MR contrast agents, such as iron nanoparticles, are currently being assessed and may be useful in detection of more subtle breaches of the BBB.

Gallagher J, Tekoriute R, O'Reilly JA, Kerskens C, Gun'ko YK and Lynch MA. (2009) Bimodal magnetic-fluorescent nanostructures for biomedical applications. J Mater Chem. 19, 4081-4084.

Corr S, Byrne S, Brougham D, Tekoriute R, Meledandri CJ, Brougham DF, Lynch MA, Kerskens C, O' Dwyer L and Gun'Ko Y, (2008) Linear assemblies of magnetic nanoparticles as MRI contrast agents. J Am Chem Soc, 130, 4214-4215

A consensus protocol for functional connectivity analysis in the rat brain

Nature Neuroscience
Resource https://doi.org/10.1038/s41593-023-01286-8

Task-free functional connectivity in animal models provides an experimental framework to examine connectivity phenomena under controlled conditions and allows for comparisons with data modalities collected under invasive or terminal procedures. Currently, animal acquisitions are performed with varying protocols and analyses that hamper result comparison and integration. Here we introduce StandardRat, a consensus rat functional magnetic resonance imaging acquisition protocol tested across 20 centers. To develop this protocol with optimized acquisition and processing parameters, we initially aggregated 65 functional imaging datasets acquired from rats across 46 centers. We developed a reproducible pipeline for analyzing rat data acquired with diverse protocols and determined experimental and processing parameters associated with the robust detection of functional connectivity across centers. We show that the standardized protocol enhances biologically plausible functional connectivity patterns relative to previous acquisitions. The protocol and processing pipeline described here is openly shared with the neuroimaging community to promote interoperability and cooperation toward tackling the most important challenges in neuroscience.

Details of author contributions and statements of data and code avail ability are available at https://doi.org/10.1038/s41593-023-01286-8

https://immalab.wordpress.com/clare-kelly/

Diffusion MRI

Diffusion MRI is a magnetic resonance imaging (MRI) method that produces *in vivo* images of biological tissues weighted with reference to the local microstructural characteristics of water diffusion. There are 2 applications which assess changes in grey matter (Diffusion Weighted MRI) and white matter (Diffusion Tensor MRI).

In **Diffusion Weighted Imaging (DWI)**, each image voxel (three dimensional pixel) has an image intensity that reflects a single best measurement of the rate of water diffusion at that location. For example, following an ischaemic stroke, cell swelling occurs; this is considered to restrict water diffusion and DWI signal enhancement occurs. DWI changes can be detected as early as 5-10 minutes following stroke and is therefore more sensitive to early changes after a stroke than more traditional MRI measurements such as T1 or T2 relaxation rates.

DWI has been used to map areas of damage following traumatic brain injury, and ischaemic stroke in animal models; these studies are ongoing. The method has also been used to assess changes in the optic nerve in a transgenic animal model of Alzheimer's Disease (which overexpresses amyloid precursor protein and presenilin 1). It is currently being assessed as a potential biomarker of age-related deterioration in function in rats and will be used to map development of changes in an animal model of multiple sclerosis.

Diffusion Tensor Imaging (DTI): Since diffusion MRI measures diffusion of water, and since molecules inside an axon move primarily along the axis of the fibre (rather than crossing the axonal membrane, especially if it is myelinated), the diffusion tensor, that can be obtained with MRI diffusion methods, contains information about spatial orientation of nerve fiber tracts (tractometry). Therefore the connectivity between different regions of the brain can be appreciated by visual inspection of such vector maps and 3D images of white matter tracts can be generated from this information.

Analysis of age-related changes in specific fibre tracts in post-mortem rat brain is ongoing. The method has also been adapted to investigate changes in blood vessels in the isolated, pulsating aorta.

The MRI suite is a national resource and for information regarding its use in your research, please contact Ciaran Conneely, Trinity College Institute of Neuroscience,
Lloyd Building, Trinity College, Dublin 2 Email:
conneec@tcd.ie
Telephone (01) 8968493

APPLICATIONS

Diffusion tensor imaging in arterial tissue: Cardiovascular Biomechanics Research Group
Lally Lab, Trinity College Dublin https://www.lallylab.eu/

Work in our lab has focused on investigating diffusion tensor imaging within arterial tissue. Initial studies highlighted the sensitivity to cell content in porcine carotid arteries – specifically that the despite maintaining native arterial tissue microstructural arrangement in decellularised arteries, the ability to measure anisotropic diffusion is lost without the presence of smooth muscle cells. [1]

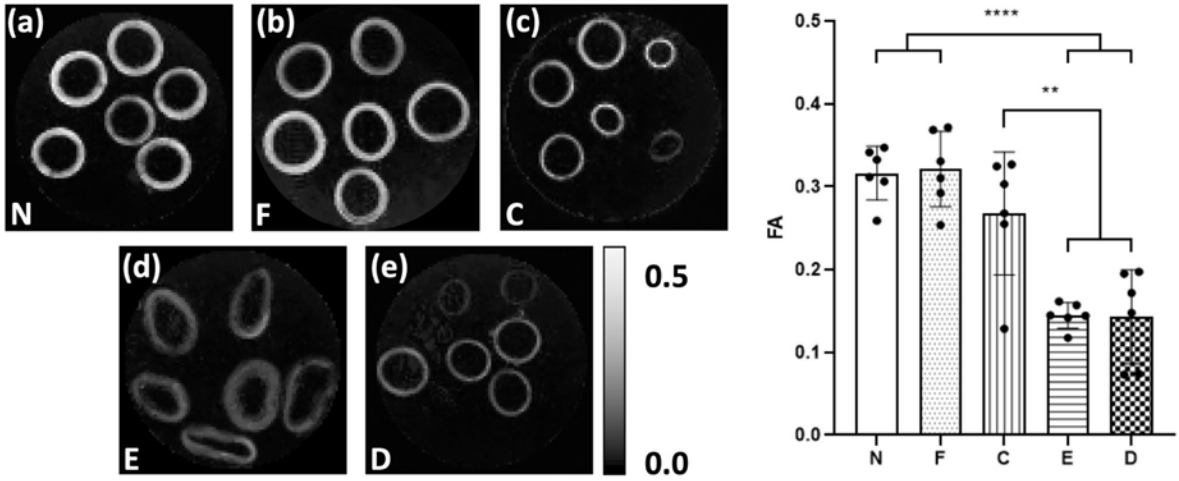

*Figure 1. Parametric maps of FA in a representative slice for each of the tissue models. As measured in vessel media, both (a) native (N) and (b) fixed native (F) PCaA showed significantly higher FA than both the (d) elastin degraded (E) and (e) decellularised (D) tissue models. (c) Collagen degraded PCaA also showed a significantly higher FA than both elastin degraded and decellularised PCaA. FA maps scaled to show 0 to 0.5 (**p =0.0018 (C vs. E), **p = 0.0016 (C vs. D), ****p<0.0001.*

Moving towards more clinically relevant human tissue, we also investigated excised human carotid arteries with varying degrees of atherosclerosis. DTI-derived metrics showed a sensitivity to early-stage atherosclerosis (the thickened intima) and late-stage (the lipid core). By combining image registration and an unsupervised segmentation algorithm, we also identified the strong correlation between elastin content and FA and MD in atherosclerotic tissue. [4]

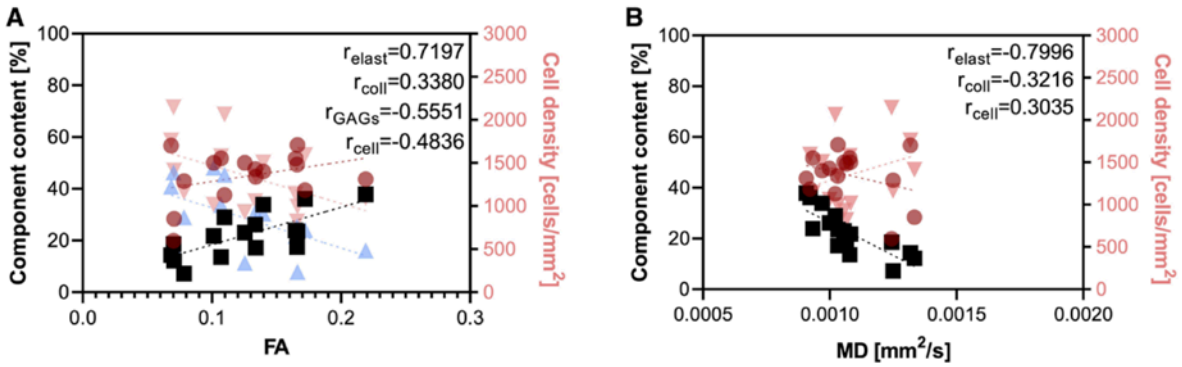

Figure 2. Correlations between microstructural components in excised human carotid arteries and DTI-derived metrics, (A) FA and (B) MD. Elastin (black squares) has a strong correlation with FA and MD, while collagen (red circles), glycosaminoglycans (blue triangles), and cell density (pink triangles) have moderate correlations with DTI-derived metrics.

We also imaged fresh excised atherosclerotic plaques prior to mechanical and histological characterisation and identified that DTI-derived tractography highlights microstructural alignments that are more, and less, vulnerable to rupture. [6]

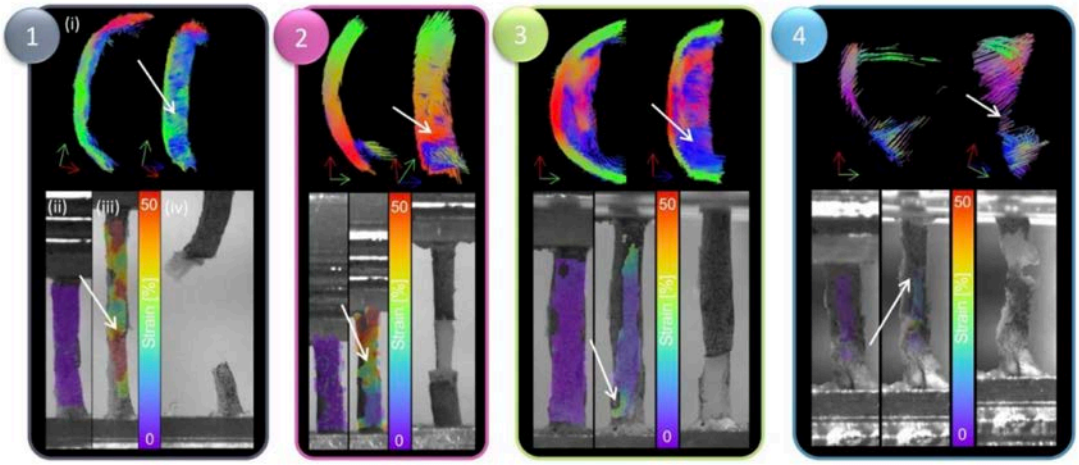

Figure 3. DIC strain contours and failure insights based on tractography groupings. For each grouping, (i) representative tractography is shown at the top, alongside strain contours on the DIC images at the (ii) reference frame (after preconditioning) and (iii) right before failure and a (iv) high-resolution image of the specimen right after failure. White arrows point to location of failure both on tractography and on strain maps.

Coming back to the initial sensitivity to cell content within arterial tissue, we also investigated tissue engineered vascular grafts. Using terminal time points and fixing the grafts on day 3, 7, and 14 of culture we imaged acellular and recellularised grafts. DTI-derived metrics, FA, MD, and tractography, can track both the recellularisation over time as well as differentiate between acellular and cellular grafts. [5]

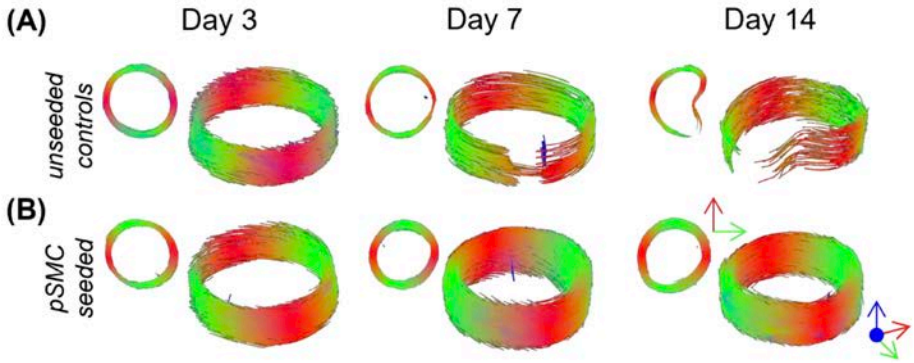

Figure 4. Tractography of tissue engineered vascular grafts. (A) Unseeded control vessels are shown in the top row, with representative (B) recellularised grafts in the second row.

Quantitative susceptibility mapping in arterial tissue: With an aim to investigate a more clinically relevant MRI sequence which is sensitive to the microstructure in arterial tissue, quantitative susceptibility mapping is also being explored within arterial tissue models. In porcine arterial tissue, a strong sensitivity to collagen content was linked to the susceptibility of the tissue. Human carotid arteries were also explored ex vivo. [3]

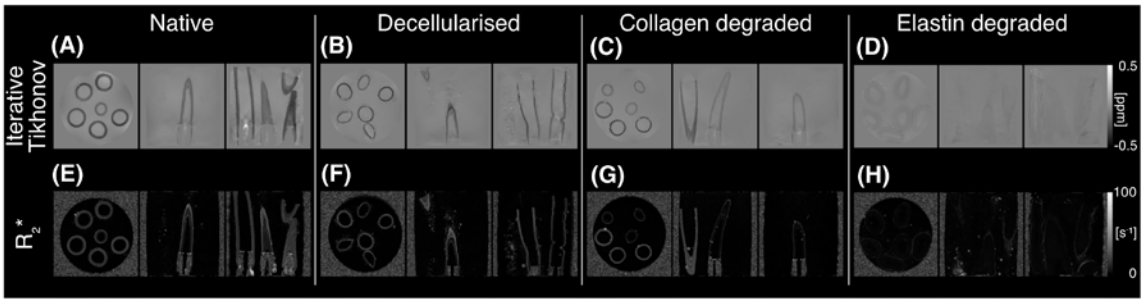

Figure 5. Susceptibility maps produced for the different porcine carotid tissue models (native, decellularised, collagen-degraded, and elastin-degraded) using the iterative Tikhonov approach (A- D) alongside maps of R∗2 (E- H).

Publications: [1] Tornifoglio, B., Stone, A. J., Johnston, R. D., Shahid, S. S., Kerskens, C., & Lally, C. (2020). Diffusion tensor imaging and arterial tissue: establishing the influence of arterial tissue microstructure on fractional anisotropy, mean diffusivity and tractography. *Scientific Reports*, *637674*, 1–12. https://doi.org/10.1038/s41598-020-77675-x

[2] Shahid, S. S., Johnston, R. D., Smekens, C., Kerskens, C., Gaul, R., Tornifoglio, B., Stone, A. J., & Lally, C. (2021). Exploring arterial tissue microstructural organization using non-Gaussian diffusion magnetic resonance schemes.

Scientific Reports, *11*(1), 1–13. https://doi.org/10.1038/s41598-021-01476-z
[3] Stone, A. J., Tornifoglio, B., Johnston, R. D., Shmueli, K., Kerskens, C., & Lally, C. (2021). Quantitative susceptibility mapping of carotid arterial tissue ex vivo: Assessing sensitivity to vessel microstructural composition. *Magnetic Resonance in Medicine*, *86*(February), 1–16. https://doi.org/10.1002/mrm.28893
[4] Tornifoglio, B., Stone, A. J., Kerskens, C., & Lally, C. (2022). Ex Vivo Study Using Diffusion Tensor Imaging to Identify Biomarkers of Atherosclerotic Disease in Human Cadaveric Carotid Arteries. *Arteriosclerosis, Thrombosis, and Vascular Biology*, *42*, 1398–1412. https://doi.org/10.1161/ATVBAHA.122.318112
[5] Tornifoglio, B., Stone, A.J., Mathieu, P. *et al.* Exploring DTI-derived metrics to non-invasively track recellularisation in vascular tissue engineering. biorxiv 2022.07.15.500196. http://doi.org/10.1101/2022.07.15.5000196; *also in submission*
[6] Tornifoglio, B., Johnston, R.D., Stone, A.J. *et al.* Microstructural and mechanical insight into atherosclerotic plaques – an ex vivo DTI study to assess plaque vulnerability. Biorxiv 2022.09.20.508689. http://doi.org/10.1101/2022.09.20.508689;
[7] Levey, R. E.*, Tornifoglio, B.*, Stone, A. J. *et al.* Towards a Whole Sample Imaging Approach Using Diffusion Tensor Imaging to Examine the Foreign Body Response to Explanted Medical Devices. Polymers (Basel). 14(22):4819. doi: 10.3390/polym14224819.

Manganese-enhanced magnetic resonance imaging (MEMRI)

Dr Oli Gobbo (Senior Research Fellow, School of Pharmacy & Pharmaceutical Sciences, TCD)
https://www.tcd.ie/research/profiles/?profile=ogobbo

Manganese-enhanced MRI (MEMRI) is being used for MRI in animals due to the unique T1 contrast that is sensitive to a number of biological processes. MEMRI relies on the complementary properties of manganese: First, it is a paramagnetic ion that affects the T1 relaxivity (1); second, it is a calcium analogue that can enter both neurons (2); and glial cells (3); and third, it can be transported along axons, can cross synapses and enter postsynaptic cells.

Current applications: The functional neural network of the animal brain, its architecture and function can be observed using MEMRI as a molecular imaging technique. Numerous uses for the paramagnetic manganese contrast in MRI exist for the visual system as well from imaging neuroprotection to assessing and monitoring neurodegeneration. Finally, MEMRI appears to be a possible effective alternative to gadolinium-enhanced MRI, for example for lung imaging.

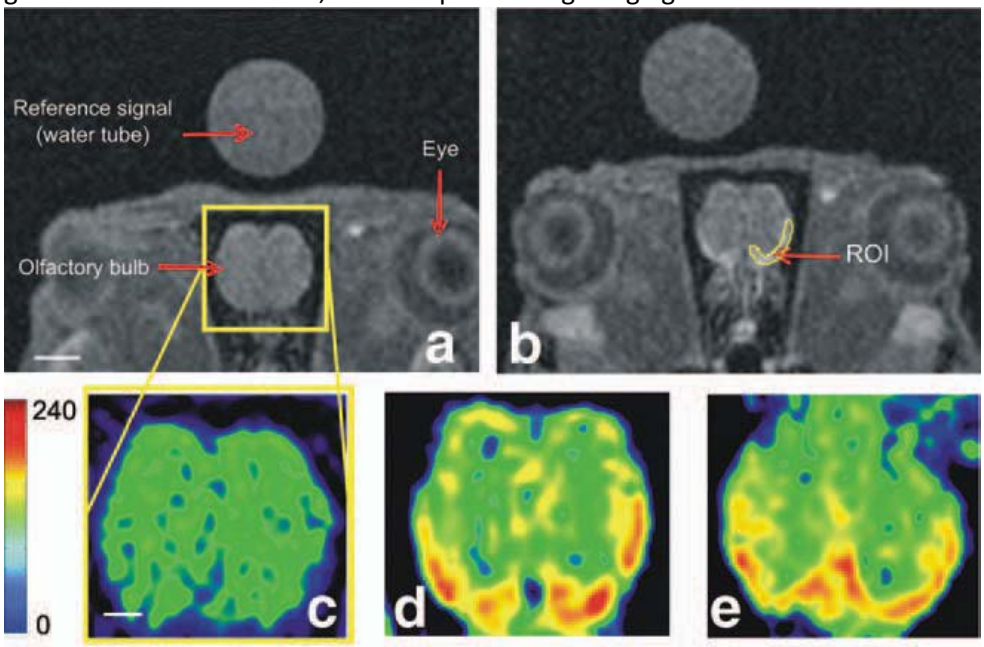

Figure 1. MEMRI signals in the rat olfactory bulb.

References:

Gobbo OL, Petit F, Gurden H, Dhenain M. In vivo detection of excitotoxicity by manganese-enhanced MRI: comparison with physiological stimulation. Magn Reson Med. 2012 Jul;68(1):234-40. doi: 10.1002/mrm.23210.
Gobbo OL, Zurek M, Tewes F, Ehrhardt C, Crémillieux Y. Manganese: a new contrast agent for lung imaging? Contrast Media Mol Imaging. 2012 Nov-Dec;7(6):542-6. doi: 10.1002/cmmi.1483.
Bianchi A, Gobbo OL, Dufort S, Sancey L, Lux F, Tillement O, Coll JL, Crémillieux Y. Orotracheal manganese-enhanced MRI (MEMRI): An effective approach for lung tumor detection. NMR Biomed. 2017 Nov;30(11). doi: 10.1002/nbm.3790
Chadderton N, Palfi A, Millington-Ward S, Gobbo O, Overlack N, Carrigan M, O'Reilly M, Campbell M, Ehrhardt C,

Wolfrum U, Humphries P, Kenna PF, Farrar G. Intravitreal delivery of AAV-NDI1 provides functional benefit in a murine model of Leber hereditary optic neuropathy. Eur J Hum Genet. 2013 Jan;21(1):62-8. doi: 10.1038/ejhg.2012.112.
Mansergh FC, Chadderton N, Kenna PF, Gobbo OL, Farrar GJ. Cell therapy using retinal progenitor cells shows therapeutic effect in a chemically-induced rotenone mouse model of Leber hereditary optic neuropathy. Eur J Hum Genet. 2014 Nov;22(11):1314-20. doi: 10.1038/ejhg.2014.26.
Boumhaouad S, Mamad O, Holmes S, Mawhinney L, Donnelly SC, Bouhaddou N, Taghzouti NK, Fayne D, Sancey L, Motto-Ros V, Crémillieux Y, Gobbo OL. In vivo detection of metastatic lung tumour using manganese-enhanced magnetic resonance imaging (under review)

2.2 Conference abstract: ISMRM 2020

Detection of lung metastases using Manganese-Enhanced MRI in an animal model

Introduction: Lung cancer is the fifth most common cancer in Ireland, with about 2,500 people diagnosed every year [1]. Lung cancer does not usually cause noticeable symptoms until it has spread through a large lung volume and/or into other organs; which is known as advanced and metastatic lung cancer. Evidently, there is an urgent medical need for an appropriate, non-invasive diagnostic tool that can detect early stage lung cancer in at-risk populations; and currently, such a technique does not exist. Our ultimate aim is to address this significant gap in oncology care, by developing a simple, easy to use diagnostic tool that can detect lung cancer at the critical early stages; thus enabling earlier therapeutic intervention and potentially improving patient prognosis. Our study confirmed that Manganese-Enhanced MRI (MEMRI) could sensitively track very small malignant neoplastic lesions in the lung [2].

Materials and Methods: The experimental protocols employed in this study were approved by the local Animal Research Ethics Committee and HPRA (Ireland), in accordance with the EU Directive (2010/63/EU). Mice received an injection of cancer cells through the tail vein. After a 3-week period, metastatic lung cancer formed in the lungs [3]. Each mouse was scanned using a preclinical 7T MRI scanner before and after an orotracheal administration of 50 µL of $MnCl_2$ at 10 mmol/L. Following the scans, the lungs were harvested for histological study in order to confirm the presence of lesions, using a Hematoxylin and Eosin (H&E) staining protocol.

Results: After orotracheal administration of $MnCl_2$, MR Images allowed the identification of potential lung metastases in all the mice (Figure 1). Histological analysis post mortem (Figure 2) has confirmed that the changes in MR signal strength after manganese administration corresponded to malignant neoplastic lesions.

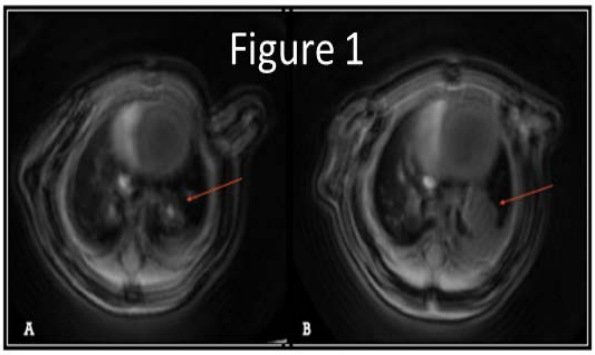

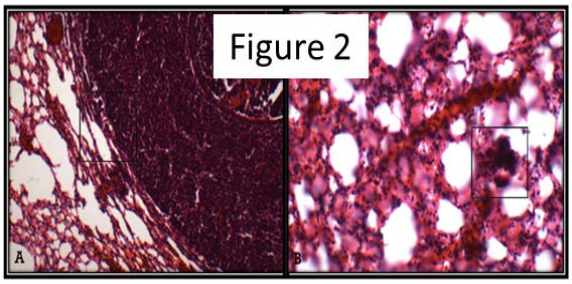

Figure 1: T1-weighted images pre (A) and post (B) nebulization of $MnCl_2$ (Cancer lesions are indicated by red arrows).

Figure 2: Histological assessment of the MRI cancer lesions in the lungs using H&E staining protocol.

Conclusion:

The results clearly demonstrated that MEMRI can be used to detect lung metastases.

References:

[1] "Cervical Cancer Awareness | Irish Cancer Society." [Online]. Available: https://www.cancer.ie/reduce-your-risk/lung-cancer-awareness#sthash.YfDJZi3r.dpbs. [Accessed: 20-Mar-2019].
[2] A. Bianchi *et al.*, *NMR Biomed.*, vol. 30, no. 11, pp. 1–10, 2017.
[3] J. J. Timmons, S. Cohessy, and E. T. Wong, "*J. Vis. Exp.*, no. 111, pp. 4–7, 2016.

Theranostic (therapy+ diagnostic) nanoparticles have the potential to completely change how diseases are treated. The creation of theranostic nanoparticles for concurrent disease imaging and therapy has garnered more attention in recent years. To address the limitations of conventional medications, several multifunctional, disease-targeted nanotheranostic systems that combine therapy and imaging in a single platform have been created. MRI provides high-resolution images of deep body structures and additional diagnostic data for more accurate characterization of the diseased site and targeted therapeutic planning.

Superparamagnetic iron oxide nanoparticles (SPIONs) play an important role in nanomedicine by serving as drug carriers and imaging agents. The development of nano-imaging through MRI also has the potential to detect and diagnose cancer at an earlier stage than current imaging methods. Full body scanning of rodents not only reveals tumour sites, but also allows visualization of the biodistribution of SPIONs, which can define their therapeutic effect and toxicity.

Fig 2. Biodistribution in vivo of superparamagnetic iron oxide nanoparticles: MRI study.

References:

Gobbo OL, Wetterling F, Vaes P, Teughels S, Markos F, Edge D, Shortt CM, Crosbie-Staunton K, Radomski MW, Volkov Y, Prina-Mello A. Biodistribution and pharmacokinetic studies of SPION using particle electron paramagnetic resonance, MRI and ICP-MS. Nanomedicine (Lond). 2015;10(11):1751-60. doi: 10.2217/nnm.15.22.

Gobbo OL, Sjaastad K, Radomski MW, Volkov Y, Prina-Mello A. Magnetic Nanoparticles in Cancer Theranostics. Theranostics. 2015 Sep 1;5(11):1249-63. doi: 10.7150/thno.11544.

Edge D, Shortt CM, Gobbo OL, Teughels S, Prina-Mello A, Volkov Y, MacEneaney P, Radomski MW, Markos F. Pharmacokinetics and bio-distribution of novel super paramagnetic iron oxide nanoparticles (SPIONs) in the anaesthetized pig. Clin Exp Pharmacol Physiol. 2016 Mar;43(3):319-26. doi: 10.1111/1440-1681.12533.

Traditionally, the Campbell lab has used the 7T MRI system at TCD for studies relating to blood-brain and blood-retina barrier (BBB/BRB) biology. Using dynamic contrast enhanced MRI (DCE-MRI), we have examined the integrity of these neural barriers in a range of animal models that have been developed by the group. These mice include models that allow us to target specific components of the BBB/BRB that can induce a transient disruption of the barrier and thereby manifesting increased gadolinium signals. In effect, the lab does not work on one disease in particular but rather allows the phenotype determined in mice dictate the clinical indication we work on. Based on results of the DCE-MRI studies, we conduct similar studies in human clinical research programs focused on epilepsy, traumatic brain injury and dementia.

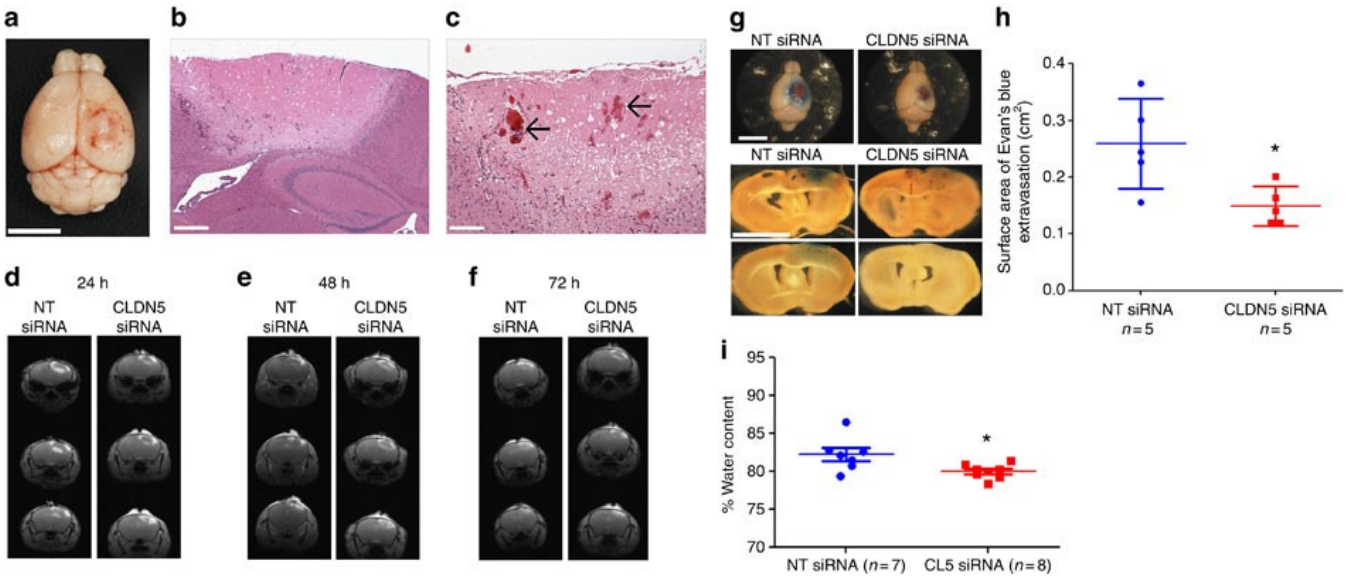

(**a**) Cold-induced cerebral injury created a focal vasogenic oedema in the right hemisphere of the mouse brain. Scale bar, 5 mm. (**b**) The focal injury extended as far as the hippocampus and created a large region of focal necrosis. Scale bar, 250 µm. (**c**) Neutrophil extravasation and endothelial cell activation are apparent along with haemmorrage (arrows). Scale bar, 100 µm. (**d**) Contrast-enhanced MRI shows the TBI region post-Gd-DTPA infusion in NT siRNA-injected mice (left panels) and claudin-5 siRNA-injected mice (right panels) 24 h post-injury. (**e**) NT siRNA-injected mice (left panel) and claudin-5 siRNA-injected mice (right panel) 48 h post-injury and (**f**) NT siRNA-injected mice (left panel) and claudin-5 siRNA-injected mice (right panel) 72 h post-injury. (**g**) Surface, cortical extravasation of Evan's blue (blue staining) was observed in NT siRNA-injected mice and claudin-5 siRNA-injected mice 48 h post-injury (left and right panels respectively; scale bar, 5 mm). Cross-sections of the injured areas were observed in both experimental groups in the panels below. Scale bars 5 mm. (**h**) Quantification of the surface area of Evan's blue extravastaion was assessed in both experimental groups (**P*=0.0464, Student's *t*-test, *n*=5 for each group). (**i**) Percentage water content as calculated by wet/dry weights was significantly decreased at the site of injury in claudin-5 siRNA-injected mice (**P*=0.0224, Student's *t*-test, NT siRNA *n*=7, claudin-5 siRNA *n*=8).

Publications

1. Hudson N, Celkova L, Hopkins A, Greene C, Storti F, Ozaki E, Fahey E, Theodoropoulou S, Kenna PF, Humphries MM, Curtis AM, Demmons E, Browne A, Liddie S, Lawrence MS, Grimm C, Cahill MT, Humphries P, Doyle SL, ***Campbell M**. Dysregulated claudin-5 cycling in the inner retina causes retinal pigment epithelial cell atrophy. ***JCI Insight***. 2019 Aug 8;4(15). **This study has described an inner retina derived initiator of pathology in AMD.**
2. Keaney, J, Walsh DM, O'Malley T, Hudson N, Crosbie DE, Loftus T, Sheehan F, McDaid J, Humphries MM, Callanan JJ, Brett FM, Farrell MA, Humphries P, ***Campbell M**. Autoregulated paracellular clearance of amyloid-β across the blood-brain barrier. ***Science Advances***. (2015) Sep

4;1(8):e1500472. **This was the first description of paracellular diffusion of amyloid-β across the BBB in the context of Alzheimer's disease.**

3. ***Campbell M**, Humphries MM, Kiang A-S, Nguyen ATH, Gobbo OL, Tam LCS, Suzuki M, Hanrahan F, Ozaki E, Farrar G-J, Kenna PF, Humphries P. Systemic low molecular weight drug delivery to pre-selected neuronal regions. ***EMBO Mol Med***, (2011), 3:235-245. **This paper describes the development and use of AAV vectors to allow for site specific modulation of the BBB/iBRB.**
4. ***Campbell, M**, Hanrahan, F, Gobbo, OL, Kelly, ME, Kiang, AS, Humphries, MM, Nguyen, ATH, Ozaki, E, Keaney, J, Blau, CW, Kerskens, CM, Cahalan, SD, Callanan, JJ, Wallace, W, Grant, GA, Doherty, CP and Humphries, P. Targeted suppression of claudin-5 decreases cerebral edema and improves cognitive outcome following traumatic brain injury. ***Nature Communications***, (2012), May 22;3:849. **This study used siRNA directed against claudin-5 to alleviate malignant cerebral edema.**

Dr Alice Whitney, Physiology Department, School of Medicine TCD

https://www.tcd.ie/research/profiles/?profile=awitney

Elucidating the complex organization of neural micro-domains in the locust Schistocerca gregaria using dMRI

To understand brain function it is necessary to characterize both the underlying structural connectivity between neurons and the physiological integrity of these connections. Previous research exploring insect brain connectivity has typically used electron microscopy techniques, but this methodology cannot be applied to living animals and so cannot be used to understand dynamic physiological processes. The relatively large brain of the desert locust, Schistercera gregaria (Forksål) is ideal for exploring a novel methodology; micro diffusion magnetic resonance imaging (micro-dMRI) for the characterization of neuronal connectivity in an insect brain. The diffusion-weighted imaging (DWI) data were acquired on a preclinical system using a customised multi-shell diffusion MRI scheme optimized to image the locust brain. Endogenous imaging contrasts from the averaged DWIs and Diffusion Kurtosis Imaging (DKI) scheme were applied to classify various anatomical features and diffusion patterns in neuropils, respectively. The application of micro-dMRI modelling to the locust brain provides a novel means of identifying anatomical regions and inferring connectivity of large tracts in an insect brain. Furthermore, quantitative imaging indices derived from the kurtosis model that include fractional anisotropy (FA), mean diffusivity (MD) and kurtosis anisotropy (KA) can be extracted. These metrics could, in future, be used to quantify longitudinal structural changes in the nervous system of the locust brain that occur due to environmental stressors or ageing.

Syed Salman Shahid, Christian M. Kerskens, Malcolm Burrows, Alice G.Witney, (2021) Elucidating the complex organization of neural micro-domains in the locust Schistocerca gregaria using dMRI, Scientific Reports, 11, (3418), 2021, p1 - 12